https://doi.org/10.5194/egusphere-2023-62
Preprint. Discussion started: 30 March 2023

Regime shift of a large river as a response to Holocene climate change depends on land use – a numerical case study from the Chinese Loess Plateau

Hao Chen[1, 2], Xianyan Wang[1*], Yanyan Yu[3], Huayu Lu[1] and Ronald Van Balen[2, 4*]

[1]Frontiers Science Center for Critical Earth Material Cycling, School of Geography and Ocean Science, Nanjing University, Nanjing 210023, China.

[2]Department of Earth Sciences, VU University Amsterdam, Amsterdam 1081HV, The Netherlands.

[3]Key Laboratory of Cenozoic Geology and Environment, Institute of Geology and Geophysics, Chinese Academy of Sciences, Beijing 100029, China.

[4]TNO-Geological Survey of the Netherlands

Correspondence to: Xianyan Wang (xianyanwang@nju.edu.cn), Ronald Van Balen (r.t.van.balen@vu.nl)

https://doi.org/10.5194/egusphere-2023-62
Preprint. Discussion started: 30 March 2023

Abstract

The Wei River catchment in the southern part of the Chinese Loess Plateau (CLP), is one of the centers of the agricultural revolution in China. The area has experienced intense land use changes since ~6000 BCE, which makes it an ideal place to study the response of fluvial systems to anthropogenic land cover change (ALCC). We applied a numerical landscape evolution model that combines the Landlab landscape evolution model with an evapotranspiration model to investigate the direct and indirect effects of ALCC on hydrological and morphological processes in the Wei River catchment since the mid-Holocene. The results show that ALCC not only leads to changes in discharge and sediment load in the catchment but also affects their sensitivity to climate change. When the proportion of agricultural land area exceeded 50% (around 1000 BCE), the sensitivities of discharge and sediment yield to climate change increased abruptly indicating a regime change in the fluvial catchment. It is associated with a large sediment pulse in the lower reaches. The model simulation results also show a link between human settlement, ALCC and floodplain development: Changes in agricultural land use changes lead to downstream sediment accumulation and floodplain development, which in turn leads to further spatial expansion of agriculture and human settlement.

Key words: Anthropogenic land cover change, fluvial regime shift, fluvial climate sensitivity, climate change, Chinese Loess Plateau, central China

https://doi.org/10.5194/egusphere-2023-62
Preprint. Discussion started: 30 March 2023

1 Introduction

Fluvial systems are affected by natural factors such as tectonics and climate change, as well as by human activities (Bridgland, 2000; Bender et al., 2016; Best, 2019; Adams et al., 2020; Bender et al., 2020; Li et al., 2020; Mossa and Chen, 2022). Many studies have focused on the changes in river systems during the last century due to human-activities, e.g. dams, reservoirs and mining (Vörösmarty et al., 2003; Brunier et al., 2014; Zhao et al., 2015; Alfieri et al., 2017; Kong et al., 2017; Webber et al., 2017; Zhang et al., 2021; Wang et al., 2022). However, human influence on the fluvial catchments can date back thousands of years, to the beginning of the local agricultural revolution (De Moor et al., 2008; Dotterweich, 2013; Ellis et al., 2016; Zhao et al., 2022a).

Recent studies have raised the possibility that increasing anthropogenic stress on a river system may increase its risk from future extreme climate events, e.g. floods and droughts, since the resilience of the river system may be reduced, thus allowing it cross a tipping point (Best and Darby, 2020; Choudhury et al., 2022). Determining the history of a river can provide insight into the effects of anthropogenic perturbations that are likely to unfold in its future evolution (Macklin and Lewin, 2019). However, the response of the fluvial catchments to external perturbations is not straightforward (Broothaerts et al., 2014; Guo et al., 2016; Verstraeten et al., 2017). Moreover, a regime shift in a fluvial catchment is difficult to notice, since gradual changes caused by

https://doi.org/10.5194/egusphere-2023-62
Preprint. Discussion started: 30 March 2023

external perturbations may alter the resilience of a fluvial catchment with only a small apparent effect on the current state (Scheffer et al., 2001). As a result, the extent to which the vulnerability of fluvial catchments is affected by human-induced changes (e.g. land use) and the moment when the threshold could be crossed remains unclear. In addition, unraveling the mechanisms governing the response of a fluvial catchment to multiple, simultaneous forcings is notoriously difficult, especially in large river systems, where external factors and their effects are unique in each catchment and even each river reach (Mao and Cherkauer, 2009; Fuller et al., 2015; Verstraeten et al., 2017; Macklin and Lewin, 2019). In consequence, a quantitative analysis of the interplay of the effects of climate change and land use change on the fluvial catchments is needed, and landscape evolution models (LEMs) provide a good opportunity for this (Zhao et al., 2022a,b).

The Chinese Loess Plateau (CLP) located in central China is affected by soil erosion seriously (Wang et al., 2006; Bloemendal et al., 2008; Zhao et al., 2013). Previous studies have already found that the erosion in the CLP is caused by both climate change and the development of agriculture which started a few thousand years ago (He et al., 2002; Huang et al., 2006; Chen et al., 2015; Chen et al., 2021). However, the exact impact of these changes and the mechanisms involved remain largely unknown, especially for the time period around 1000 BC when a sediment pulse occurred in the river system (Song et al., 2020).

The Wei River catchment, located in the southeastern part of the CLP, is one of the

https://doi.org/10.5194/egusphere-2023-62
Preprint. Discussion started: 30 March 2023

most important sediment transport routes between the CLP and the Yellow River (Fig.1). In this study, we combine the Landlab landscape evolution model (Hobley et al., 2017; Barnhart et al., 2020) with an evapotranspiration model (Thornton, 2010) to simulate the temporal and spatial changes of discharge and sediment yields in the Wei River catchment from 6000 BCE to AD 1850. In the simulations, we apply spatially and temporally varying precipitation and temperature, based on paleo-climate records (Chen et al., 2015; Peterse et al., 2011). The simulated results from KK10 scenarios produced by Kaplan et al. (2011) are used to collect the changes of anthropogenic land cover. We specifically address the fluvial regime shifts in the Wei River catchment, which are reflected by changes in the sensitivity of discharge and sediment yield to climate change due to ALCC.

2 Study area

2.1 Geographic setting

As the largest tributary of the Yellow River, the Wei River is 818 km long and has a total drainage area about 1.35×10^5 km^2 (Guo et al., 2016) (Fig. 1a). The headwaters of the river, which eventually drains into the Yellow River, are located in the Niaoshushan Mountains, in the western part of the CLP (Chang et al., 2016; Jia et al., 2021) (Fig. 1b). The Wei River catchment is located at the transitional zone of arid (north) to humid (south) areas. The catchment has an average annual precipitation of 500-700 mm and is a typical East Asian monsoon region. The precipitation mainly

https://doi.org/10.5194/egusphere-2023-62
Preprint. Discussion started: 30 March 2023

occurs from June to September (Jia et al., 2021). The mean annual temperature ranges from 7.8 ℃ to 13.5 ℃ (Tian et al., 2022). The mean annual discharge and sediment load of the Wei River are 7.5×10^9 m^3 and 3.9×10^8 t (from 1956 to 2010), respectively (Chang et al., 2016). The natural vegetation cover in the catchment changes from deciduous broadleaf forest in the east to the temperate steppe in the west (Zhou et al., 2015), and about 50% of the valley area is cultivated (Yu et al., 2016).

The northern part of the Wei River catchment is located in the southern part of the CLP and is mainly covered by loess (Liu, 1985; Li and Lu, 2010). The tributaries draining the CLP are relatively long and contribute large amounts of sediment (Fig. 1b) (Chang et al., 2016; Jia et al., 2021). The southern part of the catchment lies in the northern Qinling Mountains and has relatively short tributaries characterized by flash flows (Fig. 1b) (Jia et al., 2021). The Wei River catchment has two major tributaries, the Jing River and the Beiluo River (Fig. 1b). There are four types of landforms in the catchment: 'hilly-gully', 'rocky-hill', 'table-gully' and 'fluvial-plain' areas. These landforms also have different vegetation covers (Fig. 1c) (Yang, 2020). The 'hilly-gully area' is located in the upper reaches of the main stream of the Wei River and in the northern part of the catchment (Fig. 1c). The widely distributed steep gullies in these areas cause a significant sediment yield (Chen et al., 2016; Zhang et al., 2020; Tian et al., 2022). The 'rocky-hill area' includes the west-central and southern portions of the catchment (Fig. 1c). The drainage divide between the Jing River and the Beiluo River also belongs to this 'rocky-hill area' (Fig. 1c). It has a long history with high forest

https://doi.org/10.5194/egusphere-2023-62
Preprint. Discussion started: 30 March 2023

cover (Zhang et al., 2017). The central parts of the Jing River and Beiluo River belong to the 'table-gully area' (Fig. 1c), which is a high platform surrounded by gullies (Chen et al., 2016). The middle and lower reaches of the main stream of the Wei River belong to the 'fluvial-plain area' (Fig. 1c). They are mainly covered by alluvial deposits.

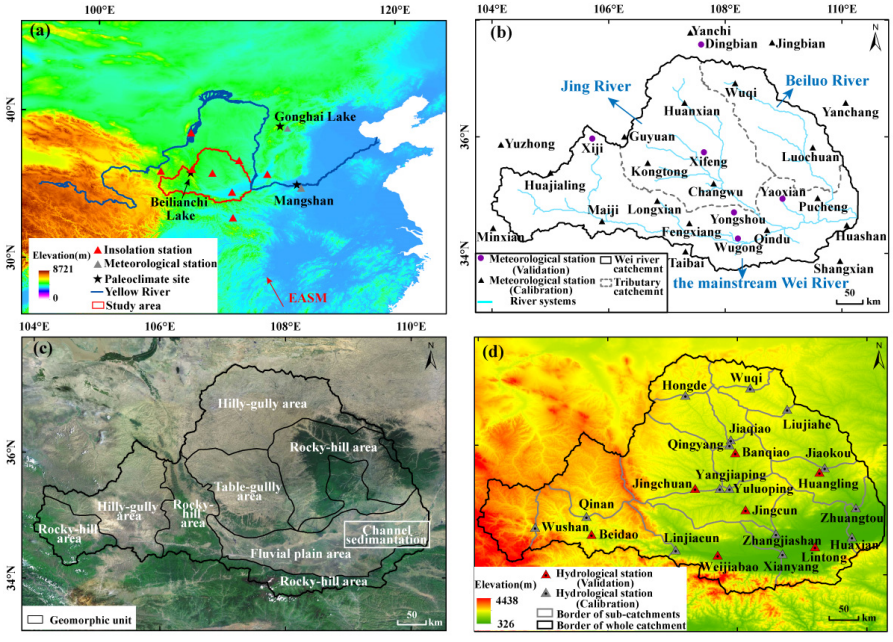

Fig 1: The Wei River catchment a. Location of the Wei River and Yellow River; b. Meteorological stations and rivers in and around the Wei River catchment; c. Landform types in the catchment; d. Hydrological stations and sub-catchments (The topographic map used in fig. 1b,d is extracted from the NASA SRTM 90m digital elevation model (https://srtm.csi.cgiar.org/); the satellite imagery used in fig. 1c is from © GoogleEarth map (https://www.earthol.com/))

https://doi.org/10.5194/egusphere-2023-62
Preprint. Discussion started: 30 March 2023

2.2 Land-use history

In China, the Yellow River basin is one of the origins of agricultural civilization (Shen, 2000). In the Wei River catchment, numerous local agricultural cultures have developed since the mid-Holocene (Table 1). Agriculture first developed at about 6000 BCE (Li et al., 2009). It started with small settlements in the southeastern part of the catchment (Laoguantai Culture; Jia, 2003) or located on the terraces of tributaries in the northerwestern part of the catchment (Dadiwan Culture; Feng, 1985). Next, during the development of the Yangshao Culture, from 5000 BCE to 3000 BCE, the intensity of agriculture and the number of settlements increased (Li et al., 2009; Tan et al., 2011). Later, the Longshan Culture, from 3000 BCE to 2000 BCE, emerged in the Wei River catchment (Jin et al., 2002). The significant increase in charcoal concentration and the diversity of food utensils during this period indicate the rapid development of an agriculture-based civilization in the catchment area (Jin et al., 2002). From 2000 BCE to 1000 BCE, the food demand of the increasing population led to further expansion of the area of agricultural land (Zhao, 2004). In addition, more high-yield crops, such as wheat, were planted in this period (pre-Zhou and Western Zhou dynasty) (Zhao, 2004). After about 1000 BCE, the intensity of agricultural activity increased significantly, with more natural vegetation being converted to crop land due to innovations in agricultural technology (Jia, 2003). From about 1000 BCE to the present, the forest cover in the Loess Plateau decreased by about 44% (Zhao et al., 2013).

https://doi.org/10.5194/egusphere-2023-62
Preprint. Discussion started: 30 March 2023

Table 1 The development of agriculture in the Wei River catchment since the mid- Holocene

(Shi, 1986; Zhou, 2003; Yu et al., 2016)

Time period	Culture	Age
6000 BCE – 5000 BCE	Laoguantai	6000 BCE – 5000 BCE
	Dadiwan	5850 BCE – 5400 BCE
5000 BCE – 4000 BCE	Yangshao	6800 BCE – 6000 BCE
4000 BCE – 3000 BCE	Yangshao	4000 BCE – 3000 BCE
	Majiayao	3600 BCE – 2900 BCE
3000 BCE – 2000 BCE	Majiayao	2900 BCE – 2050 BCE
	Longshan	2600 BCE – 2000 BCE
	Qijia	2400 BCE – 1900 BCE
2000 BCE – 1000 BCE	Siba	1900 BCE – 1500 BCE
	Kayue	1900 BCE – 1500 BCE
1000 BCE – AD 1	Xindian	1600 BCE – 600 BCE
	Siwa	1300 BCE – 500 BCE

155

2.3 Hydrology and hydrological stations

The data from twenty-two hydrological stations are used (Fig. 1d). The Wushan, Qin'an, Beidao and Linjiacun hydrological stations are located in the upper reaches of the Wei River (Fig. 1d), where the mean annual discharge and sediment load account for 26% and 30% of the entire catchment (Wang, 2013), respectively. Here, the discharge mostly originates between the Beidao and Linjiacun stations, while the sediment load is mostly produced in the upper area of the Qin'an station (Fig.1d) (Wang, 2013). The Weijiaobao, Xianyang, Lintong and Huaxian hydrological stations (Fig. 1d)

160

https://doi.org/10.5194/egusphere-2023-62
Preprint. Discussion started: 30 March 2023

are located in the middle and lower reaches of the Wei River, which contribute about 48% of the discharge of the catchment (Zhang et al., 2007). The downstream part of the Wei River, which includes the Lintong and Huaxian hydrological stations (Fig. 1d), is a typical sediment accumulation area (Gao, 2006).

The Jing River is the largest tributary of the Wei River. About 71% of its sediment is transported to the Wei River (Zhang et al., 2020). There are nine hydrological stations located in this river: the Hongde, Jiaqiao, Qingyang, Yuluoping, Jingchuan, Yangjiaping, Jingcun and the Zhangjiashan stations (Fig. 1d). The 73% of the discharge in the Jing River catchment comes from the upper reaches of the Yangjiaping station and from the reaches between the Yangjiaping, Yuluoping and Zhangjiashan stations (Zhang et al., 2020). The sediment load mainly comes from upstream of the Yuluoping station, accounting for 54% of the sediment load in the Jing River basin (Han, 2019).

For the Beiluo River, data from five hydrological stations are used in this work: the Wuqi, Liujiahe, Jiaokou, Huangling and Zhuangtou stations (Fig. 1d). The 57% of the discharge in the Beiluo River catchment is produced between the Liujiahe and Zhuangtou stations (Ran et al., 2000). Most of the sediment load is produced in the reaches upstream of the Liujiahe station, which accounts for 90.6% of the sediment load in the Beiluo River basin (Zhang et al., 2017).

https://doi.org/10.5194/egusphere-2023-62
Preprint. Discussion started: 30 March 2023

3 Materials and methods

3.1 Model development

In order to simulate the trend of fluvial sediment load and discharge under the impacts of land use and climate change, we apply the Landlab landscape model (Hobley et al., 2017; Barnhart et al., 2020) combining an evapotranspiration model (Thornton, 2010). The models are described in more detail in Chen et al.,(2021).

Simulations of the period from 1996 to 2016 are used to calibrate the model parameters by tuning the simulated discharges and sediment loads to the measured values at the hydrological stations. For simplicity, only the most important model parameters are calibrated, i.e. the effective root depth of plants and the erodibilities of the Base and Surface layers. The additional, less important parameters, such as biological parameters in the evapotranspiration model (Table S1) and the value of 'n' (a scaling exponent) in the Landlab's SPACE model component (Shobe et al., 2017) (Table S2), are provided by previous researches (Thornton, 2010; Shobe et al., 2017). Details of the calibration procedure are included in the Sect. 3.2. The calibrated model parameters are subsequently used in simulations for the time period from 6000 BCE to AD1850.

3.1.1 Evapotranspiration model

The simulated vegetation types in the Wei River catchment include deciduous broadleaf forest, grassland and crops, the distributions of which are shown in Sect. 3.3.

https://doi.org/10.5194/egusphere-2023-62
Preprint. Discussion started: 30 March 2023

Ecological parameters of deciduous broadleaf forests and grasslands are based on the default values of the Biome-BGC model (White et al., 2000; Thornton, 2010). They have previously been successfully applied to the discharge and sediment load simulations in one of the tributaries, the Beiluo River catchment (Chen et al., 2021).

For the crops, we use the winter wheat's ecological parameters since that is the dominant crop type in the Wei River catchment (Zhang et al., 1987). The soil nitrogen content, which is one of the required parameters in the model for the areas covered by crops, is assumed to be constant (0.0004kgN/m^2) to simulate the effects of fertilization (Qin et al., 2010). The crop is irrigated twice during its growth and the timing of irrigation depends on local farming practices (Zhang et al., 1987). The applied value of irrigation each year is set equal to the mean annual value of irrigation in the Wei River catchment after the 1990s (Liu, 2003). In the modelling, similar to the previous studies (Hu et al., 2011), 80% of the stems and leaves are removed each year to simulate the harvest processes.

3.1.2 Spatial distribution of climate data

For the calibration simulations of the period 1996 to 2016, we use the Kriging interpolation to compute the spatial distribution of evapotranspiration and runoff. The used meteorological data are the same as the previous simulations performed in the Beiluo River catchment (Chen et al., 2021). These data, from twenty meteorological stations located in and around the catchment (Fig. 1b), are collected from the National

https://doi.org/10.5194/egusphere-2023-62
Preprint. Discussion started: 30 March 2023

Meteorological Information Centre (http://data.cma.cn/). Eight insolation stations in and around the study area (Fig. 1a) are used to obtain the insolation data. We select another six meteorological stations (Fig. 1b) to test the accuracy of data obtained by this method. The predicted and measured data match well (R^2 > 70%, Fig. S1).

For the simulations during the Holocene (from 6000 BCE to AD 1850), the reconstructions of Holocene climate including precipitation and temperature (Peterse et al., 2011; Chen et al., 2015) are used to predict the climatic inputs, by methods of Chen et al. (2001). The predicted precipitation and air temperatures fit well with the reconstructed data in Beilianchi lake (Zhang et al., 2020, 2021) (Text S2, Fig. S2), which is located in the northwestern part of the Wei River catchment (Fig. 1a). The additional data, i.e. Holocene atmospheric CO_2 concentration, are from the results of the Vostok ice core (Barnola et al., 1995; Petit et al., 1999), while humidity and sunshine duration are set equal to modern values. Additionally, the insolation values during Holocene are calculated by the method of Laskar et al. (2004).

3.1.3 Anthropogenic land cover change

The changes of anthropogenic land use since the mid-Holocene (Fig. S3) is obtained from the KK10 database, which in turn is calculated from a global ALCC model that is driven by population density and the land suitability (Kaplan et al., 2009, 2011). The land suitability takes into account that agriculture develops first on the most productive crop lands (Kaplan et al., 2009). The simulated time series of land-use

https://doi.org/10.5194/egusphere-2023-62
Preprint. Discussion started: 30 March 2023

change for the KK10 model is from 6000 BCE to AD 1850. Only the provincial data from 221 BCE to AD 1850 are available to calibrate the spatial patterns of population changes in China (Zhao and Xie, 1988). As a result, there is an uncertainty in the land-use changes in our study region prior to 221 BC. In previous simulations focusing on the Beiluo River catchment, Chen et al. (2021) applied a variation of 25% for the ALCC from 6000 BCE to 221 BCE to estimate the impact of this uncertainty. It was shown to have a limited effect on the simulation results for discharges and sediment loads.

3.1.4 Initial topography

There are two layers in the landscape evolution model, a Base layer and a Surface layer (Shobe et al., 2017). The Surface layer consists of loose material, i.e. sediments, and is above the Base layer, which is composed of bedrock. The initial topography for the simulations is extracted from the NASA SRTM 90m digital elevation model (DEM) (https://srtm.csi.cgiar.org/) and resampled to a spatial resolution of 1000 m. Since the river network is disrupted after resampling, we resample the elevation of the network separately and combine it with the previously resampled DEM. Then, the steady-state topography is calculated over 5000 model years in order to remove DEM errors in the fluvial network (e.g. Campforts et al., 2020; Sharma et al., 2021; Chen et al., 2021). Subsequently, the elevation of the Baser layer used in the Holocene simulations is set equal to the steady-state topography. Because we use similar erodibilities of loess and sediment, the initial sediment thickness (the thickness of the Surface layer) is set to 0

https://doi.org/10.5194/egusphere-2023-62
Preprint. Discussion started: 30 March 2023

m.

3.2 Calibration

Below, we present the calibrations of model parameters by fitting the simulated discharge and sediment load to the observed values at the hydrological stations (Fig. 1d). The discharge and sediment load data from another seven hydrological stations (Fig. 1d) are used for validation. Mean annual discharge and sediment load data measured at the stations are affected by e.g. dams and irrigation systems. These data were corrected into natural discharge and sediment load data using the method by Chang et al.(2016). Details are presented in the supplemental materials (Text S1, Table S3). The calibrated parameters are the effective root depth of plants and the erodibilities of the Base and Surface layers. The calibration results are accepted when the mismatch between the simulated and observed discharges and sediment loads is less than 10%.

3.2.1 Effective root depth of plants

For the evapotranspiration model, we only calibrate the effective root depth, which is determined by the vegetation types and soil environment (Vörösmarty et al., 1989), because it has the largest impact on the evapotranspiration rates and soil water content in the evapotranspiration model.

For the root depth calibration, the catchment is subdivided into sixteen sub-catchments (Fig 1d). We use the present-day precipitation and temperature, and fit the mean annual discharge at the outlet of each sub-catchment (gray triangle in Fig. 1d).

https://doi.org/10.5194/egusphere-2023-62
Preprint. Discussion started: 30 March 2023

The initial effective root depths of plants are set at 1.5 m for deciduous broadleaf forest and 1m for grass and crop lands, based on the average root depth in the Loess Plateau (You et al., 2009). During the iterative calibration processes we vary the root depth incrementally by 1 cm, while the difference between the initial root depths of trees and grass/croplands is kept constant. After calibration, the mismatches between the observed and simulated annual discharge at the calibration stations are between 0.48% and 6.10% (Fig. S4).

In order to validate the accuracy of our calibrated results, we further compare the differences between the predicted and natural annual discharge at another seven hydrological stations (red triangle in Fig. 1d). The results show that the model predicts annual discharge with an error that ranges between 0.35% and 7.95% (Fig. S4).

3.2.2 Erodibilities

For the parameters in the Landlab model, we calibrate the erodibilities of the Base and Surface layers based on measured annual sediment loads (Fig. 1d). The initial values of the Base layer's erodibility are calculated based on the geologic map (Fig S5a), which is extracted from a 1:250,000 digital geologic map of China (Zuo et al., 2018), and the parameters of bedrock's erodibility from the LAPSUS model (Schoorl and Veldkamp, 2001). For the initial values of the Surface layer's erodibility, we calculate the values by the method of Hancock et al. (2019), which uses the soil properties and the NDVI data (Normalized Difference Vegetation Index). The data of

https://doi.org/10.5194/egusphere-2023-62
Preprint. Discussion started: 30 March 2023

soil properties (Fig. S5b-e) come from the China soil map, which in turn is collected from the Harmonized World Soil Database (v1.1) (Nachtergaele et al., 2010). The NDVI data (Fig. S5f) are based on the SPOT vegetation index database of China (http://westdc.westgis. ac.cn/).

Then, the Base layer's and Surface layer's erodibilities in each sub-catchment are adjusted until the simulated sediment load matches the observed data at the hydrological stations located at the sub-catchment's outlet (gray triangle in Fig. 1d). After calibrations, the mismatches between the observed and simulated annual sediment load at the calibration stations range from 0.01% to 9.39% (Fig. S6). For the validation stations, the model predicts annual sediment load with an error that ranges between 1.50% and 7.27% (Fig. S6).

3.3 Holocene simulations

Two model scenarios (*a model with land use and climate change, Normal, and a model without climate change, WCC*) are used in the Holocene simulations. *Scenario Normal* uses reconstructed paleo-climate data and KK10 land-use data to model the spatial and temporal changes in water and sediment discharges due to climate change and anthropogenic land cover changes. *Scenario WCC* is used to study solely the effects of land use change; the climatic conditions are kept constant.

In order to demonstrate the effects of anthropogenic land cover change on drainage hydrology, we calculate the changes of discharge and sediment yield at the outlet as

https://doi.org/10.5194/egusphere-2023-62
Preprint. Discussion started: 30 March 2023

well as their coefficient of spatial variation (CV, Eq. (1)) for the whole catchment.

$$CV = \frac{1}{x_a}\sqrt{\frac{\sum_{i=1}^{n}(x_i - x_a)^2}{n}} \quad (1)$$

Where, CV is the coefficient of spatial variation of the mean annual discharge or sediment yield. x_a is the average discharge or sediment yield of the whole catchment. x_i is the discharge or sediment yield in the i grid-cell, and n is the total number of grid-cells.

Next, the sensitivities of the mean annual discharge and sediment yield as well as their spatial variation coefficients to the climate change are calculated based on the differences between the *Normal* and *WCC* scenarios (Eq.(2)). Finally, the calculated sensitivities are correlated with the different intensities of human activity to reveal the impact of land use change on the fluvial response mechanisms.

$$S_c = \left|\frac{dif_{climate-basic}}{\Delta climate}\right| \quad (2)$$

Where, S_c is the sensitivity of the simulation results to climate change. A higher value of S_c means a more sensitive response. $dif_{climate\text{-}basic}$ is the difference between the simulation results between the *Normal* and *WCC* scenarios. The simulation results are the mean annual discharge, the CV of the mean annual discharge, the mean annual sediment yield and the CV of the mean annual sediment yield, resulting in four different sensitivity values. $\Delta climate$ is the difference between the climate conditions for the scenarios. We use the difference of precipitation between both scenarios as the $\Delta climate$ parameter, since precipitation is the climate parameter that has the most significant impact on the simulation results (Chen et al., 2021).

https://doi.org/10.5194/egusphere-2023-62
Preprint. Discussion started: 30 March 2023

In the Holocene simulation, the time-step is one year. For simplicity, the annual climatic parameters and anthropogenic land cover are set constant for each 500 years. For the modeling of discharge and sediment load, the distributions of natural plants are determined by the pollen-based reconstruction of main vegetation types in different geomorphic units in the Loess Plateau (Sun et al., 2017). By associating the reconstructed vegetation data with the modern geomorphic distribution map (http://www.geodata.cn), the natural plants in the Wei River catchment are divided into forest and grass (Fig. S7).

4 Results

4.1 *Normal scenario*

4.1.1 Runoff and discharge

The evolution of the simulated runoff and discharge from 6000 BCE to AD 1850 is shown in Fig. 2. The mean annual runoff (catchment average) increases about 16.5% during the first 2000 years (6000 BCE to 4000 BCE). A second increase of around 6.7% takes place from 2000 BCE to 500 BCE (Fig. 2A). Spatially, the simulated runoff rates show a gradual increasing trend from north to south, which is caused by the distribution of mean annual precipitation. A low value occurs in the middle reaches of the Jing River and the Beiluo River, which may be caused by the high value of effective root depth (Fig. S4) causing a locally high value of evapotranspiration.

In each sub-catchment, the fluctuations of the mean annual discharge are similar

https://doi.org/10.5194/egusphere-2023-62
Preprint. Discussion started: 30 March 2023

(Fig. 2B). The main contribution to the discharge at the catchment outlet is provided by the downstream part of the Wei River (Fig. 2b1). During the Holocene, the discharge decreases by 13.2%, 26.7%, 20.7%, 31.1%, 35.1% and 21.8% in the Wushan, Qin'an, Linjiacun, Xianyang, Huaxian and Outlet sub-catchment, respectively (Fig. 2b1). In the Jing River, the discharge decreases by 37.3%, 20.2%, 37.3%, 44.7%, 22.7% and 47.2% in the Hongde, Jiaoqiao, Qinyang, Yuluoping, Yangjiaping and Zhangjiashan sub-catchment, respectively (Fig. 2b2). In the Beiluo river, reductions about 33.1%, 29.6%, 39.9% and 50.4%, in the Wuqi, Liujiahe, Jiaokou and Zhuangtou sub-catchment, respectively (Fig.2b3).

https://doi.org/10.5194/egusphere-2023-62
Preprint. Discussion started: 30 March 2023

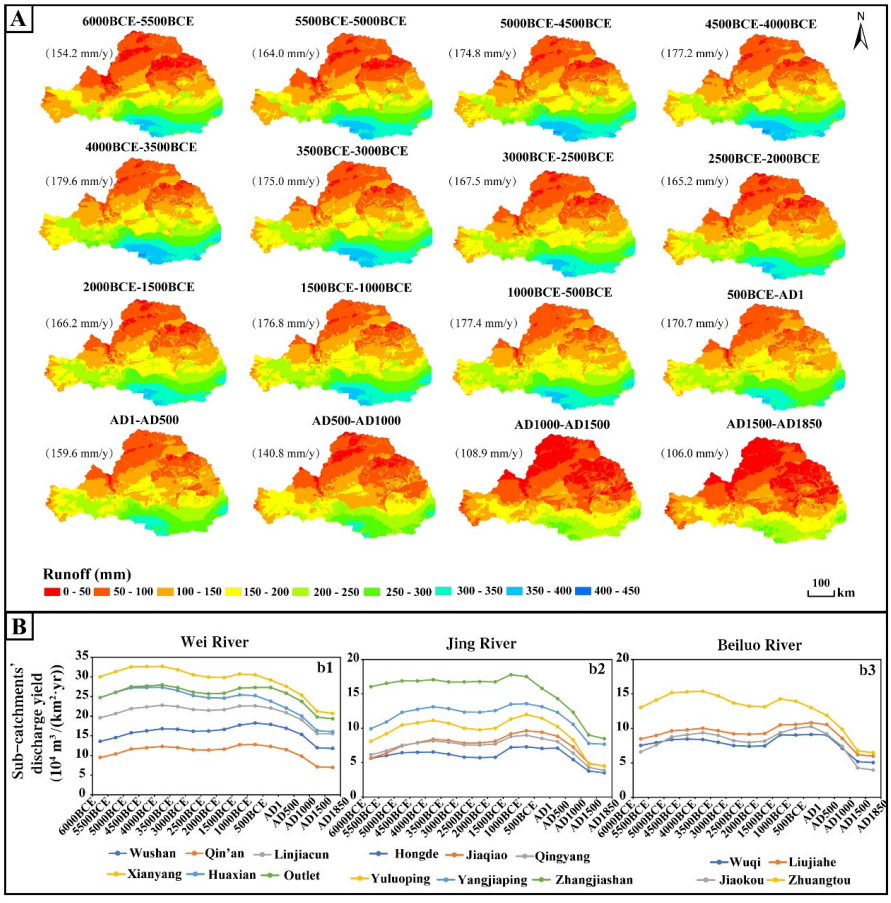

Fig 2: Simulated mean annual runoff (A) and the time-trend of sub-catchment mean annual discharge (B).

4.1.2 Sediment thickness and sediment yield

375 Figure 3 shows the distribution of sediment thickness and the evolution of sediment yield in each sub-catchment. The sediment thickness has a decreased trend from northwest to southeast. The upper and lower reaches of the main stream of the Wei River have a thin accumulation of sediment (less than 2 m) (Fig. 3A). A prominent sediment accumulation is predicted in the lower reaches from 1000 BCE onwards; its

380 lateral extension results from lateral channel migration (Fig. 3A).

https://doi.org/10.5194/egusphere-2023-62
Preprint. Discussion started: 30 March 2023

For the main stream of the Wei River, the sediment flux mainly comes from the Qin'an sub-catchment (Fig. 3b1). There is no sediment yield at the outlet of the Wei River, which indicates it is a sedimentation zone (Fig. 3b1). Sediment yields are higher in the Jing River than in other sub-catchments; the maximum value is located in the Yuluoping sub-catchment (Fig. 3b2). In the Beiluo River, the sediment is mostly produced in the Wuqi and Liujiahe sub-catchments (Fig. 3b3). The trends of mean annual sediment yield in each sub-catchment are similar and had a total increase 10 to 30 times during the simulation (Fig. 3B). Before 1000 BC, the mean annual sediment yield had an approximately steady, linear increase in all sub-catchments (Fig. 3B). Subsequently, they experienced a sharp increase between 1000 BC and AD1. Then, a rapid decrease occurred after AD 1 (Fig. 3B).

https://doi.org/10.5194/egusphere-2023-62
Preprint. Discussion started: 30 March 2023

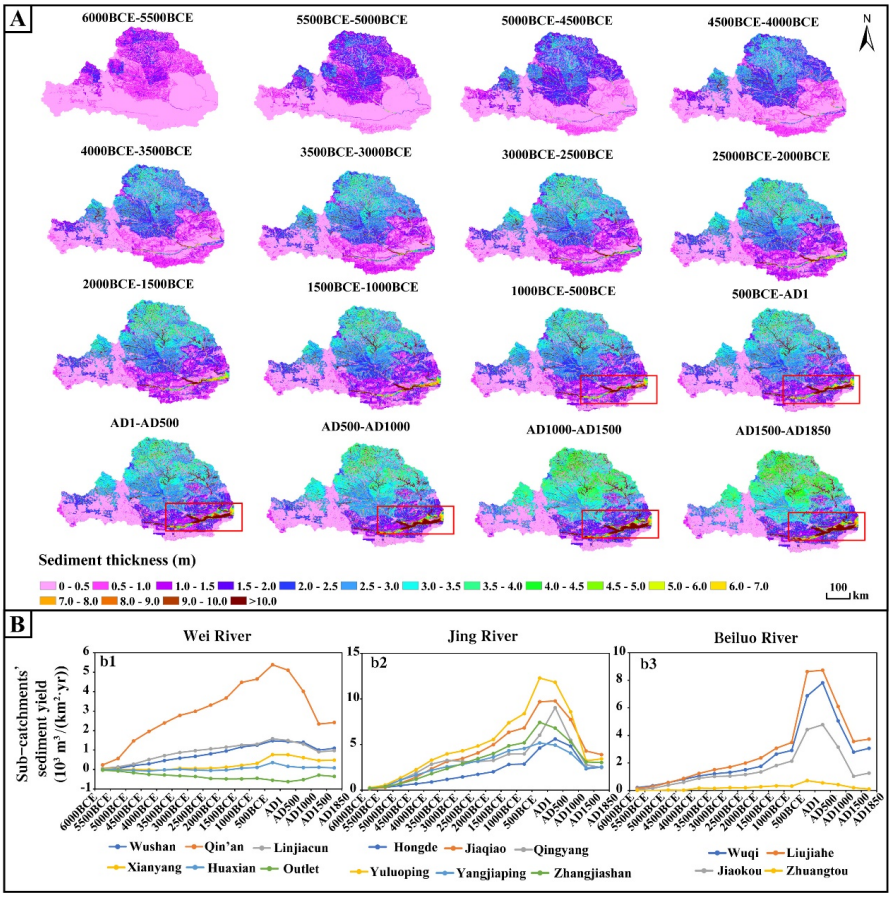

Fig 3: Sediment thickness (A) and the evolution of sub-catchment mean annual sediment yield (B)

395 4.2 The difference of model results for the two scenarios

The spatial distributions of mean annual runoff in the *Normal* and *WCC* scenarios are similar (Figs. 2A, S8A). However, the evolution of simulated mean annual runoff (catchment average) has fluctuations in the *Normal* scenario while it is almost linearly increasing in the *WCC* scenario (Figs. 2A, S8A). Compared to *Normal* scenario (Fig.

https://doi.org/10.5194/egusphere-2023-62
Preprint. Discussion started: 30 March 2023

2B), the discharge yields of the sub-catchments belonging to the southeastern part (such as Zhangjiashan and Zhuangtou) increase appreciably in the *WCC* scenario (Fig. S8B). The comparison of the mean annual discharge (catchment average) and its spatial variation coefficient for these two scenarios show that the impacts of climate change on the temporal and spatial trends of discharge start to increase after AD 1 (more than 20%) (Fig 4a, b).

In both the *Normal* and *WCC* scenarios, a large accumulation occurs in the middle reaches of Jing River at about 4000 BCE and in the downstream part of the Wei River around 1000 BCE (Figs. 3A, S9A). However, the sediment thickness in the northern part of the catchment is thicker in the *Normal* scenario than in the *WCC* scenario (Figs. 3A, S9A). In the *WCC* scenario (Fig. S9B), the sediment yields of the sub-catchments located in the northwestern part (such as Jiaoqiao, Qinyang) are larger compared to the *Normal* scenario (Fig. 3B). Based on the comparison of the results of the *Normal* scenario to those of the *WCC* scenario, the intensity of the impact of climate change on the mean annual sediment yield (in the *Normal* scenario) increases to some extent after AD 1 (more than 20%, Fig 4c). The spatial variation coefficient of sediment yield in the two scenarios are almost the same during the simulation (less than 20%, Fig 4d), which indicates that land use change is the dominant factor for the spatial characteristics of sediment yield.

https://doi.org/10.5194/egusphere-2023-62
Preprint. Discussion started: 30 March 2023

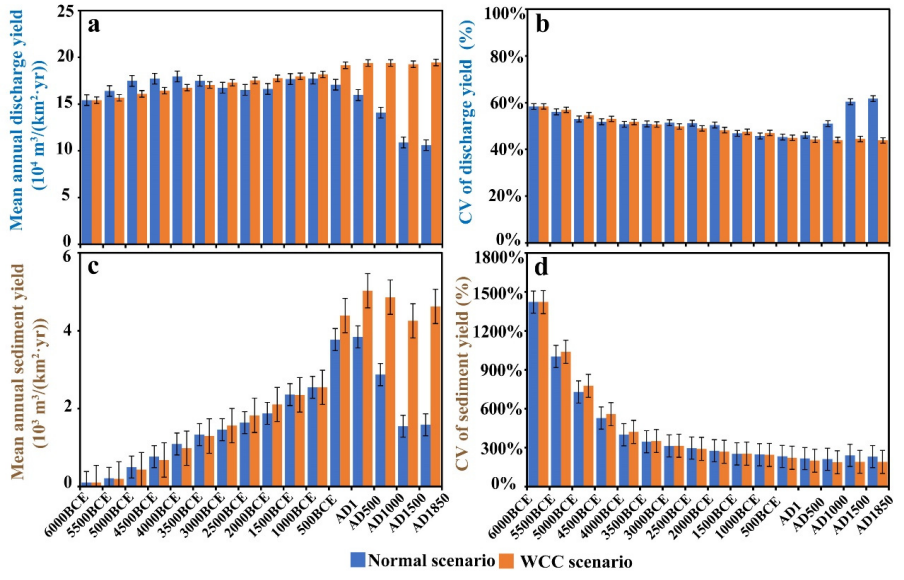

420 **Fig 4: Comparison of mean annual discharge yield (a), CV of discharge yield (b), mean annual sediment yield (c) and CV of sediment yield (d) for the *Normal* and *WCC* Scenarios**

5 Discussion

5.1 A regime shift around 1000 BC

425 The sediment thickness distribution in the *Normal* scenario shows a significant increase in the lower reaches of the main Wei River after 1000 BCE (Fig. 3A, red rectangle). The mean annual sediment yield in each sub-catchment also experiences a large increase at the same time (Fig. 3B). These changes are not only a consequence of the large increase of the land use around the 1000 BC (Chen et al., 2021), but also a 430 signal indicating the change of sensitivity of the fluvial catchment to climate change as a result of increasing ALCC.

https://doi.org/10.5194/egusphere-2023-62
Preprint. Discussion started: 30 March 2023

The sensitivity to climate change of mean annual discharge and sediment yield and their coefficient of spatial variation alters abruptly when the areal extent of land use exceeds a certain threshold (Fig. 5). When the areal extent is low (<30 %), the sensitivity to climate change declines steadily with increasing areal extent (and thus also with time; Fig. 5). The sensitivity fluctuates when the areal extent is between 30% and 50% (Fig. 5). However, when the areal extent of land use is high (>50%), starting at ~1000 BCE, the sensitivity increases with increasing areal extent (Fig. 5) indicating a regime shift of the fluvial catchment.

These changes in sensitivity are associated with the areal extent of land use and the type of vegetation change. In the catchment, the natural vegetation is made up of forest and grass (Fig. S7), which is converted to cropland. Runoff in grassland is more sensitive to climate change than runoff in cropland, whereas runoff in forest is less sensitive than runoff in cropland (Mao and Cherkauer, 2009). The main vegetation change in the catchment during the time period from 6000 BCE to around 3000 BCE is from grass to the crop in the western and northern parts of the catchment (Fig. S3), which leads to the decreased sensitivities of the catchment discharge and sediment yield and their spatial variations, CV, to climate change (Fig. 5a, b). From around 3000 BCE to 1000 BCE, the sensitivities first sharply increase and then decrease rapidly, which shows their instability. This may be caused by changes of other parameters, like air temperature (Fig. S2), which are not considered. From 1000 BCE onwards, the major anthropogenic vegetation changes are from forest to crop in the southeastern part of the

https://doi.org/10.5194/egusphere-2023-62
Preprint. Discussion started: 30 March 2023

catchment (Fig. S3), which results in the increase of the sensitivities (Fig. 5).

Sediment accumulation that first occurs in the middle reaches of the Jing River and the Beiluo River at ~ 4000 BCE, and subsequently migrates to the lower reaches of the main Wei River at ~ 1000 BCE, indicates a sediment wave, which has also been reported in other catchments (Van Balen et al., 2010; James and Lecce, 2013). Since the significant aggradation in the lower reaches of the main Wei River at ~ 1000 BCE reflects a regime shift of the whole fluvial catchment, the earlier sediment accumulation in the middle reaches of the Jing River and the Beiluo River at ~ 4000 BCE maybe indicate an earlier regime shift in the tributaries.

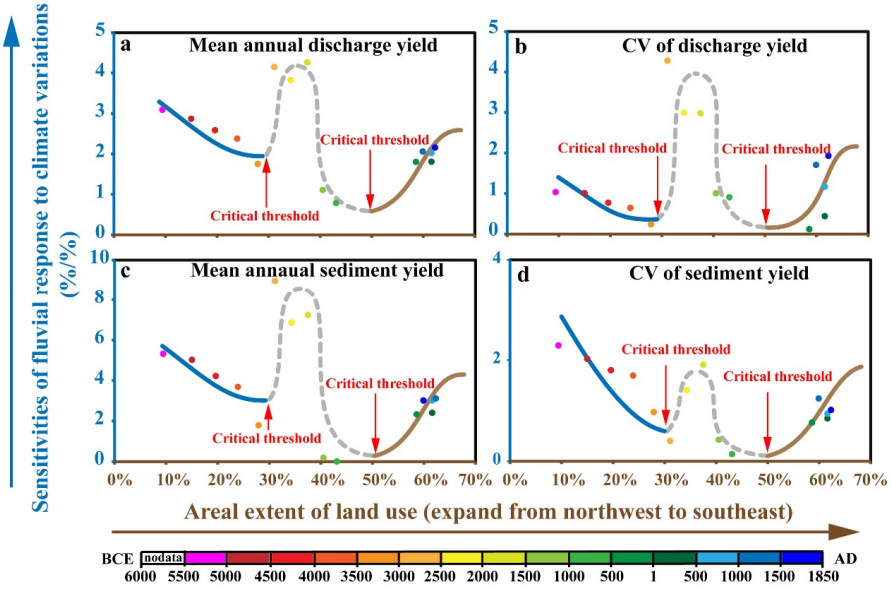

Fig 5: Sensitivity of discharge and sediment yield to the climate changes due to increasing areal extent of land use with time. The colors of points indicate the simulated time; 50% land use area corresponds to 1000 BCE.

https://doi.org/10.5194/egusphere-2023-62
Preprint. Discussion started: 30 March 2023

5.2 Coupling between ALCC by human settlement and floodplain development

The spatial distribution of sediment accumulation correlates with the distribution of archaeological sites since the mid-Holocene (Yu et al., 2016; Fig. 6). Sediment accumulation and floodplain construction first occurs in the downstream part, then expands to the northwestern part and becomes concentrated in the upstream part in the western part of the CLP, in the Qi'an and Yangjiaping sub-catchments (Fig. 6a). This pattern of expansion is consistent with the spatial trend of the growth of the number of archaeological sites during the same period (Yu et al., 2016). This can be explained by the spatially asynchronous development of floodplains, caused by migration of sediment waves in the catchment. The floodplains provided ideal locations for initial settlements (Clevis et al., 2006). These new settlements, in turn, would have led to an increase in local land use, which in turn, would result in higher sediment yields. These sediments are then transported further and accumulated downstream, which results in floodplain development there and thus provides new suitable places for further human settlement (Fig. 7). This resembles the niche construction theory (NCT) from biological and ecological systems (Laland et al., 1996; Laland et al., 1999; Laland et al., 2001; O'Brien and Laland, 2012). The NCT places emphasis on the capacity of organisms, in this case humans, to modify their environment and thereby act as co-directors of their own, and other species' evolution (Laland et al., 2001; Spengler, 2021).

https://doi.org/10.5194/egusphere-2023-62
Preprint. Discussion started: 30 March 2023

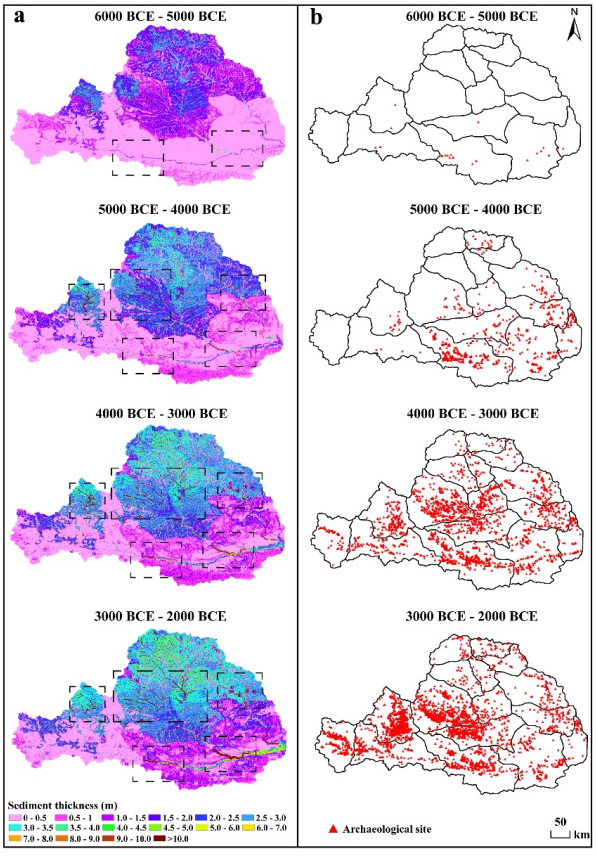

485 **Fig 6: The spatial correspondence between the location of sediment aggradation (a) and archaeological sites (b, Yu et al., 2016) during the mid-Holocene.**

https://doi.org/10.5194/egusphere-2023-62
Preprint. Discussion started: 30 March 2023

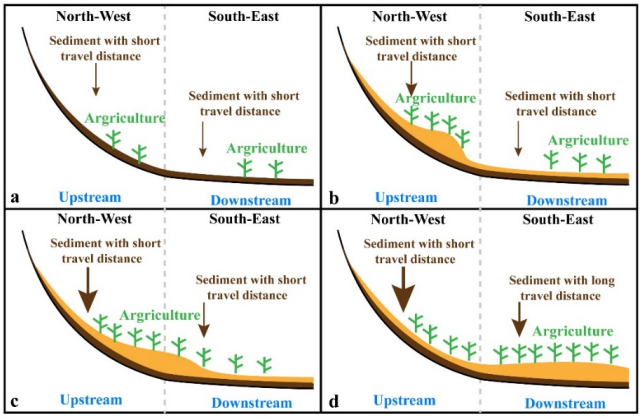

Fig 7: Conceptual model for the relationship between expansion of agriculture and fluvial floodplain aggradation.

6 Conclusions

Land use change in the Wei River catchment in the Chinese Loess Plateau (CLP) not only has a significant direct impact on discharge and sediment yield, but also alters the resilience of this fluvial catchment to climate change. The sensitivity of the entire catchment to climate change decreases with increasing amounts of areal extent of land use, as long as it is less than 30%, when the increase in areal extent is dominated by a change from grass to cropland. The sensitivity increases when the areal extent of land use exceeds 50% of the catchment around 1000 BCE. During this increase in extent, the main vegetation cover changed from trees to crops. This regime shift can be reflected by the significant sediment accumulation in the lower reaches starting around 1000 BCE. There is an initial sediment aggradation in the middle reaches of Jing River and Beiluo River (~ 4000 BCE), which migrates to the lower part of Wei River around

https://doi.org/10.5194/egusphere-2023-62
Preprint. Discussion started: 30 March 2023

3000 years ago. This migration of sedimentary waves suggests that the regime shifts occur earlier upstream in the tributaries. Our simulation results also suggest that there is a coupling between early land use, sediment accumulation and resultant floodplain development: new settlements on floodplains lead to further increases in sediment yield and floodplain formation further downstream.

Code and data availability

The mapped shapefiles and the code used to process the mapped data are available upon request to the corresponding author. The data for the KK10 scenario can be accessed at https://doi.pangaea.de/10.1594/PANGAEA.871369. The documentation of the Landlab can be found at https://landlab.readthedocs.io/ and the newest version of the software is archived at https://doi.org/10.5281/zenodo.3647556 and https://doi.org/10.5281/zenodo.3644240. The source of Biome-BGC model can be accessed at http://www.ntsg.umt.edu.

Author contribution

Hao Chen wrote the code and performed the simulations. Xianyan Wang and Ronald van Balen modified the code and improved the simulations. Yanyan Yu provided the data of archaeological sites. Huayu Lu modified the main text of the manuscript. Hao Chen wrote the manuscript with contributions from all co-authors.

Competing interests

The authors declare that they have no conflict of interest.

https://doi.org/10.5194/egusphere-2023-62
Preprint. Discussion started: 30 March 2023

Acknowledgements

We appreciate Professor Jed O Kaplan for providing the anthropogenic land cover change data simulated by the KK10 model. We also thank Professor Kuang xueyuan for the simulated paleo-climate results from CESM model. This research is supported by the National Natural Science Foundation of China (42021001, 41971005), Second Tibetan Plateau Scientific Expedition Program (2019QZKK0205).

References

Adams, B., Whipple, K., Forte, A., Heimsath, A. and Hodges, K.: Climate controls on erosion in tectonically active landscapes, Science Advances, 6(42), eaaz3166, http://doi.org/10.1126/sciadv.aaz3166, 2020.

Alfieri, L., Bisselink, B., Dottori, F., Naumann, G., de Roo, A., Salamon, P., Wyser, K. and Feyen, L.: Global projections of river flood risk in a warmer world, Earth's Future, 5(2), 171-182, http://doi.org/10.1002/2016EF000485, 2017.

Barnhart, K. R., Hutton, E. W. H., Tucker, G. E., Gasparini, N. M. and Bandaragoda, C.: Short communication: Landlab v2.0: a software package for Earth surface dynamics, Earth Surface Dynamics, 8(2), 379-397, http://doi.org/10.5194/esurf-8-379-2020, 2020.

Barnola, J. M., Anklin, M., Porcheron, J., Raynaud, D., Schwander, J. and Stauffer, B.: CO2 evolution during the last millennium as recorded by Antarctic and Greenland ice, Tellus B: Chemical and Physical Meteorology, 47(1-2), 264-272, http://doi.org/10.1034/j.1600-0889.47.issue1.22.x, 1995.

Bender, A. M., Amos, C. B., Bierman, P., Rood, D. H., Staisch, L., Kelsey, H. and Sherrod, B.: Differential uplift and incision of the Yakima River terraces, central Washington State, Journal of Geophysical Research: Solid Earth, 121(1), 365-384, http://doi.org/10.1002/2015JB012303, 2016.

Bender, A. M., Lease, R. O., Corbett, L. B., Bierman, P. R., Caffee, M. W. and Rittenour, T. M.: Late Cenozoic climate change paces landscape adjustments to Yukon River capture, Nature Geoscience, 13(8), 571-575, http://doi.org/10.1038/s41561-020-0611-4, 2020.

Best, J.: Anthropogenic stresses on the world's big rivers, Nature Geoscience, 12(1), 7-21, http://doi.org/10.1038/s41561-018-0262-x, 2019.

Best, J. and Darby, S. E.: The pace of human-induced change in large rivers: Stresses, resilience, and vulnerability to extreme events, One Earth, 2(6), 510-514,

https://doi.org/10.5194/egusphere-2023-62
Preprint. Discussion started: 30 March 2023

http://doi.org/10.1016/j.oneear.2020.05.021, 2020.

Bloemendal, J., Liu, X., Sun, Y. and Li, N.: An assessment of magnetic and geochemical indicators of weathering and pedogenesis at two contrasting sites on the Chinese Loess plateau, Palaeogeography, Palaeoclimatology, Palaeoecology, 257(1-2), 152-168, http://doi.org/10.1016/j.palaeo.2007.09.017, 2008.

Bridgland, D. R.: River terrace systems in north-west Europe: an archive of environmental change, uplift and early human occupation, Quaternary Science Reviews, 19(13), 1293-1303, http://doi.org/10.1016/S0277-3791(99)00095-5, 2000.

Broothaerts, N., Notebaert, B., Verstraeten, G., Kasse, C., Bohncke, S. and Vandenberghe, J.: Non-uniform and diachronous Holocene floodplain evolution: a case study from the Dijle catchment, Belgium, Journal of Quaternary Science, 29(4), 351-360, http://doi.org/10.1002/jqs.2709, 2014.

Brunier, G., Anthony, E. J., Goichot, M., Provansal, M. and Dussouillez, P.: Recent morphological changes in the Mekong and Bassac river channels, Mekong delta: The marked impact of river-bed mining and implications for delta destabilisation. Geomorphology, 224, 177-191, http://doi.org/10.1016/j.geomorph.2014.07.009, 2014.

Campforts, B., Shobe, C. M., Steer, P., Vanmaercke, M. and Braun, J.: HyLands 1.0: a Hybrid Landscape evolution model to simulate the impact of landslides and landslide-derived sediment on landscape evolution, Geoscientific Model Development, 13(9), 3863-3886, http://doi.org/10.5194/gmd-13-3863-2020, 2020.

Chang, J., Li, Y., Wei, J., Wang, Y. and Guo, A.: Dynamic changes of sediment load and water discharge in the Weihe River, China, Environmental Earth Sciences, 75(12), 1-17, http://doi.org/10.1007/s12665-016-5841-9, 2016.

Chen, F., Xu, Q., Chen, J., Birks, H. J. B., Liu, J., Zhang, S., Jin, L., An, C., Telford, R., Cao, X., Wang, Z., Zhang, X., Selvaraj, K., Lu, H., Li, Y., Zheng, Z., Wang, H., Zhou, A., Dong, G., Zhang, J., Huang, X., Bloemendal, J. and Rao, Z.: East Asian summer monsoon precipitation variability since the last deglaciation, Scientific Reports, 5, 11186, http://doi.org/10.1038/srep11186, 2015.

Chen, H., Wang, X., Lu, H. and Van Balen, R.: Anthropogenic impacts on Holocene fluvial dynamics in the Chinese Loess Plateau, an evaluation based on landscape evolution modeling, Geomorphology, 392, 107935, http://doi.org/10.1016/j.geomorph.2021.107935, 2021.

Chen, N., Ma, T. and Zhang, X.: Responses of soil erosion processes to land cover changes in the Loess Plateau of China: A case study on the Beiluo River basin, Catena, 136, 118-127, http://doi.org/10.1016/j.catena.2015.02.022, 2016.

Chen, Y., Wang, K., Lin, Y., Shi, W., Song, Y. and He, X.: Balancing green and grain trade, Nature Geoscience, 8(10), 739-741, http://doi.org/10.1038/ngeo2544, 2015.

Choudhury, M., Pervez, A., Sharma, A. and Mehta, J.: Human-induced stresses on the rivers beyond their assimilation and regeneration capacity Ecological Significance

https://doi.org/10.5194/egusphere-2023-62
Preprint. Discussion started: 30 March 2023

of River Ecosystems (pp. 281-298): Elsevier, 2022..

Clevis, Q., Tucker, G. E., Lock, G., Lancaster, S. T., Gasparini, N., Desitter, A. and Bras, R. L.: Geoarchaeological simulation of meandering river deposits and settlement distributions: A three-dimensional approach, Geoarchaeology: An International Journal, 21(8), 843-874, http://doi.org/10.1002/gea.20142, 2006.

Crutzen, P. and Stoermer, E.: The "Anthropocene", Global Change Newsl, 41, 17–18, http://www.igbp.net/download/18.316f18321323470177580001401/1376383088452/NL41.pdf, 2000.

Crutzen, P. J.: Geology of mankind, Nature, 415(6867), 23, http://doi.org/10.1007/978-3-319-27460-7_10, 2002.

De Moor, J., Kasse, C., Van Balen, R., Vandenberghe, J. and Wallinga, J.: Human and climate impact on catchment development during the Holocene—Geul River, the Netherlands, Geomorphology, 98(3-4), 316-339, http://doi.org/10.1016/j.geomorph.2006.12.033, 2008.

Dotterweich, M.: The history of human-induced soil erosion: Geomorphic legacies, early descriptions and research, and the development of soil conservation—A global synopsis, Geomorphology, 201, 1-34, http://doi.org/10.1016/j.geomorph.2013.07.021, 2013.

Ellis, E., Maslin, M., Boivin, N. and Bauer, A.: Involve social scientists in defining the Anthropocene, Nature, 540(7632), 192-193, https://doi.org/10.1038/540192a, 2016.

Feng, S.: Origin of Chinese agriculture as viewed from Daliwan cultural relics, Acta Geographica Sinica, 40(3):207-214, http://doi.org/10.11821/xb198503002, 1985.

Fuller, I. C., Macklin, M. G. and Richardson, J. M.: The Geography of the Anthropocene in N ew Z ealand: Differential River Catchment Response to Human Impact, Geographical Research, 53(3), 255-269, http://doi.org/10.1111/1745-5871.12121, 2015.

Fuller, M. R., Doyle, M. W. and Strayer, D. L.: Causes and consequences of habitat fragmentation in river networks, Annals of the New York Academy of Sciences, 1355(1), 31-51, https://doi.org/10.1111/nyas.12853, 2015.

Jia, Y.: Study on the Holocene environmental change in the Eastern region of Guanzhong basin and its influence on human culture—a case study on loess profile in Laoguantai, M.S. thesis, Shaanxi Normal University (In Chinese), 2003.

Gao, W.: Effects of water and sediment of Jing Rvier on the deformation of riverbed of Wei River, M.S. thesis, Xi'an University of Technology (In Chinese), 2006..

Guo, A., Chang, J., Wang, Y. and Huang, Q.: Variations in the runoff-sediment relationship of the Weihe River basin based on the copula function, Water, 8(6), 223, http://doi.org/10.3390/w8060223, 2016.

Han, X.: Spatial and temporal variation of runoff and sediment in Jing River basin and the influencing factors, M.S. thesis, Southwest University (In Chinese), 2019.

Hancock, G. R., Wells, T., Dever, C. and Braggins, M.: Hillslope and point based soil

https://doi.org/10.5194/egusphere-2023-62
Preprint. Discussion started: 30 March 2023

erosion–an evaluation of a Landscape Evolution Model, Earth Surface Processes and Landforms, 44(5), 1163-1177, http://doi.org/10.1002/esp.4566, 2019.

He, X., Tang, K., Matthews, J. A. and Owen, G.: Erosion response to anthropogenic activity and climatic changes during the Holocene: case studies in northwestern China and southern Norway, Journal of Geographical Sciences, 12(4), 467-471, http://doi.org/doi.org/10.1007/BF02844605, 2002.

Hobley, D. E. J., Adams, J. M., Siddhartha Nudurupati, S., Hutton, E. W. H., Gasparini, N. M., Istanbulluoglu, E. and Tucker, G. E.: Creative computing with Landlab: an open-source toolkit for building, coupling, and exploring two-dimensional numerical models of Earth-surface dynamics, Earth Surface Dynamics, 5, 21-46, http://doi.org/10.5194/esurf-5-21-2017, 2017.

Hu, B., Sun, R., Chen, Y., Feng, L. and Sun, L.: Estimation of the net ecosystem productivity in Huang-Huai-Hai region combining with Biome-BGC model and remote sensing data, Journal of Natural Resources, 26(12), 2061-2071, http://doi.org/10.11849/zrzyxb.2011.12.006 (In Chinese), 2011.

Huang, C., Jia, Y., Pang, J., Zha, X. and Su, H.: Holocene colluviation and its implications for tracing human-induced soil erosion and redeposition on the piedmont loess lands of the Qinling Mountains, northern China, Geoderma, 136(3-4), 838-851, http://doi.org/0.1016/j.geoderma.2006.06.006, 2006.

James, L. and Lecce, S.: Impacts of land-use and land-cover change on river systems, Treatise on geomorphology, 9, 768-793, http://doi.org/10.1016/B978-0-12-374739-6.00264-5, 2013.

Jia, H., Qu, W., Ren, W. and Qian, H.: Impacts of chemical weathering and human perturbations on dissolved loads of the Wei River, the Yellow River catchment, Journal of Hydrology, 603, 126950, http://doi.org/10.1016/j.jhydrol.2021.126950, 2021.

Jin, R., Li, Y. and Ma, Z.: The historical geography background of Chinese civilization origin on Guan-zhong area, Journal of Tianjin Normal University (Social Science), 161(2), 35-42, http://doi.org/10.3969/j.issn.1671-1106.2002.02.008 (In Chinese), 2002.

Kaplan, J. O., Krumhardt, K. M., Ellis, E. C., Ruddiman, W. F., Lemmen, C. and Goldewijk, K. K.: Holocene carbon emissions as a result of anthropogenic land cover change, Holocene, 21(5), 775-791, https://doi.org/10.1177/0959683610386983, 2011.

Kaplan, J. O., Krumhardt, K. M. and Zimmermann, N.: The prehistoric and preindustrial deforestation of Europe, Quaternary Science Reviews, 28(27–28), 3016-3034, http://doi.org/10.1016/j.quascirev.2009.09.028, 2009.

Kong, D., Miao, C., Wu, J., Borthwick, A. G., Duan, Q. and Zhang, X.: Environmental impact assessments of the Xiaolangdi Reservoir on the most hyperconcentrated laden river, Yellow River, China, Environmental Science and Pollution Research, 24(5), 4337-4351, http://doi.org/10.1007/s11356-016-7975-4, 2017.

https://doi.org/10.5194/egusphere-2023-62
Preprint. Discussion started: 30 March 2023

Laland, K. N., Odling-Smee, F. J. and Feldman, M. W.: Evolutionary consequences of niche construction and their implications for ecology, Proceedings of the National Academy of Sciences, 96(18), 10242-10247, http://doi.org/10.1073/pnas.96.18.10242, 1999.

Laland, K. N., Odling-Smee, F. J. and Feldman, M. W.: The evolutionary consequences of niche construction: a theoretical investigation using two-locus theory, Journal of evolutionary biology, 9(3), 293-316, http://doi.org/10.1046/j.1420-9101.1996.9030293.x, 1996.

Laland, K. N., Odling-Smee, J. and Feldman, M. W. Cultural niche construction and human evolution, Journal of evolutionary biology, 14(1), 22-33, http://doi.org/10.1046/j.1420-9101.2001.00262.x, 2001.

Laskar, J., Robutel, P., Joutel, F., Gastineau, M., Correia, A. C. M. and Levrard, B.: A long-term numerical solution for the insolation quantities of the Earth, Astronomy & Astrophysics, 428(1), 261-285, http://doi.org/10.1051/0004-6361:20041335, 2004.

Lewis, S. L. and Maslin, M. A.: Defining the anthropocene, Nature, 519(7542), 171, http://doi.org/10.1038/nature14258, 2015.

Li, L. and Lu, H.: A preliminarily quantitative estimation of the sedimentation and erosion rates of loess deposits in Chinese Loess Plateau over the past 250 ka, Acta Geographica Sinica, 65(1), 37-52, http://doi.org/10.1017/S0004972710001772, 2010.

Li, P., zhang, Y., Ma, D., Yao, W., Holden, J., Irvine, B. and Zhao, G.: Soil erosion rates assessed by RUSLE and PESERA for a Chinese Loess Plateau catchment under land - cover changes, Earth Surface Processes and Landforms, 45, 707-722, http://doi.org/10.1002/esp.4767, 2020.

Li, X., Xue, S., Dodson, J. and Zhou, X.: Holocene agriculture in the Guanzhong Basin in NW China indicated by pollen and charcoal evidence, Holocene, 19(8), 1213-1220, http://doi.org/10.1177/0959683609345083, 2009.

Liu, D.: Loess and Environment (D. Liu Ed.), Beijing: China Ocean Press, 1985.

Liu, H.: Analysis of the conditions and trends of water and sediment in the Weihe River basin, M.S. thesis, Xi'an University of Technology (In Chinese), 2003.

Macklin, M. G. and Lewin, J.: River stresses in anthropogenic times: Large-scale global patterns and extended environmental timelines, Progress in Physical Geography: Earth and Environment, 43(1), 3-23, http://doi.org/10.1177/0309133318803013, 2019.

Mao, D. and Cherkauer, K. A., Impacts of land-use change on hydrologic responses in the Great Lakes region, Journal of Hydrology, 374(1-2), 71-82, http://doi.org/10.1016/j.jhydrol.2009.06.016, 2009.

Mossa, J. and Chen, Y.: Geomorphic response to historic and ongoing human impacts in a large lowland river, Earth Surface Processes and Landforms, 1-20, http://doi.org/10.13140/RG.2.2.32716.82566, 2022.

https://doi.org/10.5194/egusphere-2023-62
Preprint. Discussion started: 30 March 2023

Nachtergaele, F., Van Velthuizen, H., Verelst, L., Batjes, N., Dijkshoorn, K., Van Engelen, V., Fischer, G., Jones, A., Montanarella, L., Petri, M., Prieler, S., Shi, X., Teixeira, E. and Wiberg, D.: The harmonized world soil database, Paper presented at the The 19th World Congress of Soil Science, Soil Solutions for a Changing World, Brisbane, Australia, 1-6 August 2010, 34-37, 2010.

O'Brien, M. J. and Laland, K. N.: Genes, culture, and agriculture: An example of human niche construction, Current Anthropology, 53(4), 434-470, http://doi.org/10.1086/666585, 2012.

Peterse, F., Prins, M. A., Beets, C. J., Troelstra, S. R., Zheng, H., Gu, Z., Schouten, S. and Damste, S.: Decoupled warming and monsoon precipitation in East Asia over the last deglaciation, Earth & Planetary Science Letters, 301(1-2), 256-264, http://doi.org/10.1016/j.epsl.2010.11.010, 2011.

Petit, J. R., Jouzel, J., Raynaud, D., Barkov, N. I., Barnola, J. M., Basile, I., Bender. M., Chappellaz, J., Davis, M., Delaygue, G., Delmotte, M., Kotlyakov, V. M., Legrand, M., Lipenkov, V. Y., Lorius, C., Pepin, L., Ritz, C., Saltzman, E. and Stievenard, M.: Climate and atmospheric history of the past 420,000 years from the Vostok ice core, Antarctica, Nature, 399(6735), 429-436, http://doi.org/10.1038/20859, 1999.

Qin, Z., Su, G., Zhang, J., Ouyang, Y., Yu, Q. and Li, J.: Identification of important factors for water vapor flux and CO2 exchange in a cropland, Ecological modelling, 221(4), 575-581, http://doi.org/10.1016/j.ecolmodel.2009.11.007, 2010.

Ran, D., Liu, L., Zhao, L., Bai, Z., Liu, B. and Wang, H.: The soil conservation practices and streamflow and sediment load changes in the Hekou-Longmen region of middle reaches of Yellow River (L. Zhao Ed.), Zhengzhou, China: Yellow River Water Conservancy Press (in Chinese), 2000.

Scheffer, M., Carpenter, S., Foley, J. A., Folke, C. and Walker, B.: Catastrophic shifts in ecosystems, Nature, 413(6856), 591-596, http://doi.org/10.1038/35098000, 2001.

Schoorl, J. M. and Veldkamp, A.: Linking land use and landscape process modelling: a case study for the Alora region (south Spain), Agriculture, ecosystems & environment, 85(1-3), 281-292, http://doi.org/10.1016/S0167-8809(01)00194-3, 2001.

Sharma, H., Ehlers, T. A., Glotzbach, C., Schmid, M. and Tielbörger, K.: Effect of rock uplift and Milankovitch timescale variations in precipitation and vegetation cover on catchment erosion rates, Earth Surface Dynamics, 9(4), 1045-1072, http://doi.org/10.5194/esurf-9-1045-2021, 2021.

Shen, Z.: Developmental stages of primitive agriculture in China (in Chinese), Agricultural History of China, 19(2), 3-9, 2000.

Shi, X.: Yangshao culture. In: Archaeological Editorial Committee (ed.) Encyclopedia of China (Archaeology), Beijing: Encyclopedia of China Publishing House (in Chinese), 1986.

https://doi.org/10.5194/egusphere-2023-62
Preprint. Discussion started: 30 March 2023

Shobe, C. M., Tucker, G. E. and Barnhart, K. R.: The SPACE 1.0 model: a Landlab component for 2-D calculation of sediment transport, bedrock erosion, and landscape evolution, Geoscientific Model Development, 10(12), 1-38, http://doi.org/10.5194/gmd-2017-175, 2017.

Song, S., Wang, S., Fu, B., Liu, Y., Wang, K., Li, Y. and Wang, Y.: Sediment transport under increasing anthropogenic stress: Regime shifts within the Yellow River, China, Ambio, 49(12), 2015-2025, http://doi.org/10.1007/s13280-020-01350-8, 2020.

Spengler, R. N.: Niche Construction Theory in archaeology: A critical review, Journal of Archaeological Method and Theory, 28(3), 925-955, https://doi.org/10.1007/s10816-021-09528-4, 2021.

Sun, A., Guo, Z., Wu, H., Qin, L. and Li, X.: Reconstruction of the vegetation distribution of different topographic units of the Chinese Loess Plateau during the Holocene, Quaternary Science Reviews, 173, 236-247, http://doi.org/10.1016/j.quascirev.2017.08.006, 2017.

Tan, Z., Huang, C., Pang, J. and Zhou, Q.: Holocene wildfires related to climate and land-use change over the Weihe River Basin, China, Quaternary International, 234(1-2), 167-173, http://doi.org/10.1016/j.quaint.2010.03.008, 2011.

Thornton, P. E.: Biome-BGC version 4.2: Theoretical framework of Biome-BGC, Technical documentation, 2010.

Tian, P., Liu, L., Tian, X., Zhao, G., Klik, A., Wang, R., Lu, X., Mu, X. and Bai, Y.: Sediment yields variation and response to the controlling factors in the Wei River Basin, China, Catena, 213, 106181, http://doi.org/10.1016/j.catena.2022.106181, 2022.

Van Balen, R., Busschers, F. S. and Tucker, G. E.: Modeling the response of the Rhine–Meuse fluvial system to Late Pleistocene climate change, Geomorphology, 114(3), 440-452, http://doi.org/10.1016/j.geomorph.2009.08.007, 2010.

Verstraeten, G., Broothaerts, N., Van Loo, M., Notebaert, B., D'Haen, K., Dusar, B. and De Brue, H.: Variability in fluvial geomorphic response to anthropogenic disturbance, Geomorphology, 294, 20-39, http://doi.org/10.1016/j.geomorph.2017.03.027, 2017.

Vörösmarty, C. J., Meybeck, M., Fekete, B., Sharma, K., Green, P. and Syvitski, J. P.: Anthropogenic sediment retention: major global impact from registered river impoundments, Global and Planetary Change, 39(1-2), 169-190, http://doi.org/10.1016/S0921-8181(03)00023-7, 2003.

Vörösmarty, C. J., Moore III, B., Grace, A. L., Gildea, M. P., Melillo, J. M., Peterson, B. J., Rastetter, E. B. and Steudler, P. A.: Continental scale models of water balance and fluvial transport: An application to South America, Global biogeochemical cycles, 3(3), 241-265, http://doi.org/10.1029/GB003i003p00241, 1989.

Wang, L., Shao, M., Wang, Q. and Gale, W. J.: Historical changes in the environment of the Chinese Loess Plateau, Environmental science & policy, 9(7-8), 675-684,

https://doi.org/10.5194/egusphere-2023-62
Preprint. Discussion started: 30 March 2023

http://doi.org/10.1016/j.envsci.2006.08.003, 2006.

Wang, S.: Variation and regularity of water and sediment characteristics in the upper reaches of Wei River (In Chinese), Water Resources Planning and Design, (9), 8-10, http://doi.org/10.3969/j.issn.1672-2469.2013.09.003, 2013.

Wang, Z., Xu, M., Liu, X., Singh, D. K. and Fu, X.: Quantifying the impact of climate change and anthropogenic activities on runoff and sediment load reduction in a typical Loess Plateau watershed, Journal of Hydrology: Regional Studies, 39, 100992, http://doi.org/10.1016/j.ejrh.2022.100992, 2022.

Waters, C. N., Zalasiewicz, J., Summerhayes, C., Barnosky, A. D., Poirier, C., Gałuszka, A., Cearreta, A., Edgeworth, M., Ellis, E. C. Eills, M., Jeandel, C., Leinfelder, R., McNeill, J. R. Richter, D., Steffen, W., Syvitski, J., Vidas, D., Wagreich, M., Williams, M., An, Z., Grinevald, J., Odada, E., Oreskes, N. and Wolfe, A. P.: The Anthropocene is functionally and stratigraphically distinct from the Holocene, science, 351, aad2622, http://doi.org/10.1126/science.aad2622, 2016.

Webber, M., Crow-Miller, B. and Rogers, S.: The South–North water transfer project: Remaking the geography of China, Regional Studies, 51(3), 370-382, http://doi.org/10.1080/00343404.2016.1265647, 2017.

White, M. A., Thornton, P. E., Running, S. W. and Nemani, R. R.: Parameterization and Sensitivity Analysis of the BIOME–BGC Terrestrial Ecosystem Model: Net Primary Production Controls, Earth Interactions, 4(3), 1-84, http://doi.org/10.1175/1087-3562(2000)0042.0.CO;2, 2000.

Yang, J.: Analysis and driving attribution of hydrological variation transfer law in Wei River basin, M. S. thesis, Changan University (In Chinese), 2020

You, S., Di, S. and Yuan, Y.: Study on soil field capacity estimation in the Loess Plateau region (In Chinese), Journal of Natural Resources, 24(3), 545-552, http://doi.org/10.11849/zrzyxb.2009.03.020, 2009.

Yu, Y., Wu, H., Finke, P. A. and Guo, Z.: Spatial and temporal changes of prehistoric human land use in the Wei River valley, northern China, The Holocene, 26(11), 1788-1801, http://doi.org/10.1177/0959683616645943, 2016.

Zalasiewicz, J., Waters, C. and Williams, M.: The anthropocene Geologic Time Scale 2020 (pp. 1257-1280), Elsevier, 2020.

Zhang, C., Zhao, C., Yu, Z., Zhang, H., Zhou, A., Zhang, X., Feng, X., Sun, X. and Shen, L.: Western Pacific Ocean influences on monsoon precipitation in the southwestern Chinese Loess Plateau since the mid-Holocene, Climate Dynamics, 54(5), 3121-3134, http://doi.org/10.1007/s00382-020-05159-9, 2020.

Zhang, C., Zhao, C., Zhou, A., Zhang, H. and Chen, F.: Quantification of temperature and precipitation changes in northern China during the "5000-year" Chinese History, Quaternary Science Reviews, 255(11186), 106819, http://doi.org/10.1016/j.quascirev.2021.106819, 2021.

Zhang, F., Wang, D. and Qiu, B.: Agricultural Phenology Atlas of China, Beijing: Science press (In Chinese), 1987.

https://doi.org/10.5194/egusphere-2023-62
Preprint. Discussion started: 30 March 2023

Zhang, G., Ding, W., Liu, H., Yi, L., Lei, X. and Zhang, O.: Quantifying climatic and anthropogenic influences on water discharge and sediment load in Xiangxi River Basin of the three gorges reservoir area, Water Resources, 48(2), 204-218, http://doi.org/10.1134/S0097807821020184, 2021.

Zhang, H., Zhao, H., Gu, M. and Zhang, H.: Analysis of variation of water and sediment of Weihe basin in Shaanxi province (In Chinese), Journal of Yangling Vocational & Technical College, 6(2), 1-4, http://doi.org/10.3969/j.issn.1671-9131.2007.02.001, 2007.

Zhang, J., Shang, Y., Liu, J., Fu, J., Wei, S. and Tong, L.: Causes of variations in sediment yield in the Jinghe River Basin, China, Scientific Reports, 10(1), 1-18, http://doi.org/10.1038/s41598-020-74980-3, 2020.

Zhang, J., Zhang, X., Li, R., Chen, L. and Lin, P.: Did streamflow or suspended sediment concentration changes reduce sediment load in the middle reaches of the Yellow River, Journal of Hydrology, 546, 357-369, http://doi.org/10.1016/j.jhydrol.2017.01.002, 2017.

Zhao, G., Mu, X., Wen, Z., Wang, F. and Gao, P.: Soil erosion, conservation, and eco-environment changes in the Loess Plateau of China, Land Degradation & Development, 24(5), 499-510, http://doi.org/10.1002/ldr.2246, 2013.

Zhao, H., Lin, Y., Delang, C. O., Ma, Y., Zhou, J., and He, H.: Contribution of soil erosion to the evolution of the plateau-plain-delta system in the Yellow River basin over the past 10,000 years, Palaeogeography, Palaeoclimatology, Palaeoecology, 601, 111133, http://doi.org/10.1016/j.palaeo.2022.111133, 2022a.

Zhao, H., Lin, Y., Zhou, J., Delang, C. O. and He, H.: Simulation of Holocene soil erosion and sediment deposition processes in the Yellow River basin during the Holocene, Catena, 219, 106600, http://doi.org/10.1016/j.catena.2022.106600, 2022b.

Zhao, W. and Xie, S.: History of Population in China (Zhong guo Ren Kou Shi), Beijing, China: People's Publishing House, 1988.

Zhao, Y., Zou, X., Gao, J., Xu, X., Wang, C., Tang, D., Wang, T. and Wu, X.: Quantifying the anthropogenic and climatic contributions to changes in water discharge and sediment load into the sea: A case study of the Yangtze River, China, Science of the Total Environment, 536, 803-812, http://doi.org/10.1016/j.scitotenv.2015.07.119, 2015.

Zhao, Z.: The elementary analysis of the floating sieving result from the Zhouyuan site (Wangjiazui site) (in Chinese), Cultural Relic, 10, 89-96, 2004.

Zhou, J., Zhang, C. and Xie, X.: Vegetation net primary productivity temporal and spatial patterns and influence factors analysis in Weihe watershed (In Chinese), Journal of Soil and Water Conservation, 29(2), 274-277, http://doi.org/10.13870/j.cnki.stbcxb.2015.02.051, 2015.

Zhou, Q. High-resolution Studies of the evolution of pedogenic environment and effect of human activity during Holocene in the Weihe valley, Ph. D. thesis, Shaanxi

https://doi.org/10.5194/egusphere-2023-62
Preprint. Discussion started: 30 March 2023

885 Normal University (In Chinese), 2003.

Zuo, Q., Ye, T., Feng, Y., Ge, Z. and Qang, Y. Spatial database of 1 : 250000 construction and structure maps in mainland China (In Chinese), Geology of China, 45(S1), 1-26&130-163, 2018.